

Non-Hermitian Perturbations to the Fritzsch Textures of Lepton and Quark Mass Matrices

Harald Fritzsch[‡], Zhi-zhong Xing^{† *}, Ye-Ling Zhou[†]

[†]Institute of High Energy Physics, Chinese Academy of Sciences, Beijing 100049, China

[‡]Physik-Department, Universität München, D-80333 Munich, Germany

Abstract

We show that non-Hermitian and nearest-neighbor-interacting perturbations to the Fritzsch textures of lepton and quark mass matrices can make both of them fit current experimental data very well. In particular, we obtain $\theta_{23} \simeq 45^\circ$ for the atmospheric neutrino mixing angle and predict $\theta_{13} \simeq 3^\circ$ to 6° for the smallest neutrino mixing angle when the perturbations in the lepton sector are at the 20% level. The same level of perturbations is required in the quark sector, where the Jarlskog invariant of CP violation is about 3.7×10^{-5} . In comparison, the strength of leptonic CP violation is possible to reach about 1.5×10^{-2} in neutrino oscillations.

PACS number(s): 14.60.Pq, 13.10.+q, 25.30.Pt

Keywords: quark and lepton masses, flavor mixing, Fritzsch texture

*E-mail: xingzz@ihep.ac.cn

1 Introduction

The flavor sector in the standard model (SM) of electroweak interactions has been puzzling because it involves most of the free parameters of the model itself. Although the values of six quark masses and those of three angles and one CP-violating phase of the 3×3 Cabibbo-Kobayashi-Maskawa (CKM) quark mixing matrix V [1] are all known to a good degree of accuracy [2], it remains very difficult to understand why they have the observed mass spectrum and flavor mixing pattern. The situation in the lepton sector is even worse: not only the absolute mass scale of three neutrinos but also the smallest angle and CP-violating phases of the 3×3 Maki-Nakagawa-Sakata-Pontecorvo (MNSP) lepton mixing matrix U [3] are still unknown. To resolve the flavor problem in the SM one has to gain an insight into the flavor structures and possible flavor symmetries behind them. In spite of many attempts in this direction, a successful (unique and predictive) flavor theory has not been achieved. Most of the present-day studies on the flavor structures of quarks and leptons are more or less phenomenological [4], and among them the texture-zero approach [5] has proved to be very useful to establish some simple and testable relations between the mass ratios of quarks or leptons and their corresponding flavor mixing angles.

In the three-family framework the Fritzsch texture of quark mass matrices [6]

$$M_\alpha^{(\text{F})} = \begin{pmatrix} 0 & A_\alpha & 0 \\ A_\alpha^* & 0 & B_\alpha \\ 0 & B_\alpha^* & C_\alpha \end{pmatrix}, \quad (1)$$

where $\alpha = \text{u}$ (up) or d (down), has attracted a lot of interest since it was proposed in 1978. It belongs to the more generic nearest-neighbor-interaction (NNI) form of quark mass matrices,

$$M_\alpha^{(\text{NNI})} = \begin{pmatrix} 0 & A_\alpha & 0 \\ A'_\alpha & 0 & B_\alpha \\ 0 & B'_\alpha & C_\alpha \end{pmatrix}. \quad (2)$$

The NNI form can always be obtained from an arbitrary form of M_u and M_d via a proper choice of the flavor basis in the SM [7]. So the Fritzsch texture is actually a NNI texture with the additional assumption of the Hermiticity conditions $A'_\alpha = A_\alpha^*$ and $B'_\alpha = B_\alpha^*$. In view of the problem that $M_\text{u}^{(\text{F})}$ and $M_\text{d}^{(\text{F})}$ cannot simultaneously give rise to a sufficiently large value of the top-quark mass m_t and a sufficiently small value of the CKM matrix element $|V_{cb}|$, one has to abandon either the NNI feature of quark mass matrices [8] or their Hermiticity [9], either partly or completely¹. It is always possible to numerically determine the departures of realistic M_u and M_d from $M_\text{u}^{(\text{F})}$ and $M_\text{d}^{(\text{F})}$ by using current experimental data. If such departures are not very significant, they can be regarded as small perturbations and then be treated in an analytical way so that their effects on the CKM matrix elements will become more transparent.

It also makes sense to consider non-Hermitian and nearest-neighbor-interacting perturbations to the Fritzsch-type lepton mass matrices $M_l^{(\text{F})}$ and $M_\nu^{(\text{F})}$. Although the latter can fit current experimental data [10], it is very difficult to obtain $\theta_{23} \simeq 45^\circ$ or equivalently the maximal or nearly maximal atmospheric neutrino mixing. One possible way out is to introduce the seesaw

¹One may certainly abandon both the NNI and Hermiticity conditions by following a different starting point of view (e.g., the triangular form of M_u and M_d) to investigate quark mass matrices and their consequences on flavor mixing and CP violation [4]. But we do not focus on this possibility in the present work.

mechanism to the neutrino sector [11], in which the Dirac neutrino mass matrix M_D takes the Fritzsch texture as M_l does but the heavy Majorana neutrino mass matrix M_R is (approximately) proportional to the identity matrix. Here we follow a different way at the electroweak scale. We shall introduce non-Hermitian perturbations to both $M_l^{(F)}$ and $M_\nu^{(F)}$ so that the resultant charged-lepton and neutrino mass matrices can agree with current neutrino oscillation data to a better degree of accuracy². Such a parallel study of lepton and quark mass matrices of approximate Fritzsch textures is useful to reveal the similarities and differences between the lepton and quark sectors, and it should also be helpful for building a unified flavor model of leptons and quarks.

Let us point out that the present work is different from a recent one done by Branco *et al* [12] in the following three aspects. (1) They have only considered quark mass matrices of the NNI form, whereas we are discussing both lepton and quark mass matrices of the same NNI form and giving a stronger emphasis to the lepton sector. In particular, we are concerned about an interpretation of the observed $\theta_{23} \simeq 45^\circ$ and a prediction of nonzero θ_{13} for the MNSP matrix based on the NNI texture of lepton mass matrices at the electroweak scale. (2) The analytical approximations made in our perturbative calculation are valid to a better degree of accuracy and thus allow one to see the difference between the contribution of fermion mass ratios and that of perturbation parameters (which signify a departure of the NNI texture from Hermiticity) to the flavor mixing matrix elements in a clearer way. (3) Our numerical analysis is more comprehensive than the one done in Ref. [12], and it shows that current experimental data require the non-Hermitian effects to be at the 20% level in both lepton and quark sectors. This observation is expected to be useful for model building, especially when leptons and quarks are discussed in a unified flavor picture.

The remaining part of this paper is organized as follows. In section 2 we do a perturbative calculation to reveal the salient features of non-Hermitian corrections to the Fritzsch textures of lepton and quark mass matrices. Section 3 is devoted to a numerical illustration of the constrained parameter space at a reasonable level of perturbations in the lepton and quark sectors. A brief summary, together with some further discussions, is given in section 4.

2 A perturbative calculation

Without loss of generality, the NNI mass matrix $M_\alpha^{(\text{NNI})}$ (for $\alpha = u, d, l$ or ν) in Eq. (2) can always be decomposed into $M_\alpha^{(\text{NNI})} = P_\alpha \tilde{M}_\alpha^{(\text{NNI})} P'_\alpha$, where P_α and P'_α are two independent diagonal phase matrices, and

$$\tilde{M}_\alpha^{(\text{NNI})} = \begin{pmatrix} 0 & a_\alpha & 0 \\ a'_\alpha & 0 & b_\alpha \\ 0 & b'_\alpha & c_\alpha \end{pmatrix} \quad (3)$$

is real. After the bi-unitary transformation $O_\alpha^\dagger \tilde{M}_\alpha^{(\text{NNI})} O'_\alpha = \widehat{M}_\alpha \equiv \text{Diag}\{\lambda_1^\alpha, \lambda_2^\alpha, \lambda_3^\alpha\}$ with λ_i^α (for $i = 1, 2, 3$) being three mass eigenvalues, we can obtain the CKM and MNSP matrices as follows:

$$\begin{aligned} V &= (P_u O_u)^\dagger (P_d O_d) = O_u^\dagger P_V O_d, \\ U &= (P_l O_l)^\dagger (P_\nu O_\nu) = O_l^\dagger P_U O_\nu, \end{aligned} \quad (4)$$

²In this treatment we have assumed massive neutrinos to be the Dirac particles because the overall neutrino mass matrix M_ν is not symmetric. Of course, one may first apply the same treatment to M_D and then invoke the seesaw mechanism to produce a Majorana mass matrix M_ν for three light neutrinos.

where $P_V \equiv P_u^\dagger P_d = \text{Diag}\{e^{i\phi_1}, e^{i\phi_2}, 1\}$ and $P_U \equiv P_l^\dagger P_\nu = \text{Diag}\{e^{i\varphi_1}, e^{i\varphi_2}, 1\}$ are two diagonal phase matrices in a chosen phase convention.

Following the same model-building strategy as specified in Ref. [12], here we focus on the consequences of $M_\alpha^{(\text{NNI})}$ on flavor mixing. We consider the real mass matrix $\tilde{M}_\alpha^{(\text{NNI})} = \tilde{M}_\alpha^{(\text{F})} + \tilde{M}_\alpha^{(\epsilon)}$, where

$$\begin{aligned}\tilde{M}_\alpha^{(\text{F})} &= \begin{pmatrix} 0 & a_\alpha & 0 \\ a_\alpha & 0 & b_\alpha \\ 0 & b_\alpha & c_\alpha \end{pmatrix}, \\ \tilde{M}_\alpha^{(\epsilon)} &= \begin{pmatrix} 0 & -a_\alpha \epsilon_a^\alpha & 0 \\ +a_\alpha \epsilon_a^\alpha & 0 & -b_\alpha \epsilon_b^\alpha \\ 0 & +b_\alpha \epsilon_b^\alpha & 0 \end{pmatrix}\end{aligned}\quad (5)$$

with ϵ_a^α and ϵ_b^α being dimensionless real parameters describing small and asymmetric corrections to $\tilde{M}_\alpha^{(\text{F})}$. Treating ϵ_a^α and ϵ_b^α as perturbation parameters will technically allow us to perform an analytical diagonalization of $\tilde{M}_\alpha^{(\text{NNI})}$. For simplicity, we omit the flavor index α in the subsequent discussions. It is easy to exactly diagonalize $\tilde{M}^{(\text{NNI})} = \tilde{M}^{(\text{F})}$ in the limit of $\epsilon_a = \epsilon_b = 0$ [13]:

$$\begin{aligned}a &= \sqrt{\frac{\lambda_1 \lambda_2 \lambda_3}{(\lambda_1 - \lambda_2 + \lambda_3)}}, \\ b &= \sqrt{\frac{(\lambda_1 - \lambda_2)(\lambda_2 - \lambda_3)(\lambda_1 + \lambda_3)}{\lambda_1 - \lambda_2 + \lambda_3}}, \\ c &= \lambda_1 - \lambda_2 + \lambda_3;\end{aligned}\quad (6)$$

and

$$\begin{aligned}O_{11}^{(0)} &= \sqrt{\frac{\lambda_2 \lambda_3 (\lambda_3 - \lambda_2)}{(\lambda_1 + \lambda_2)(\lambda_1 - \lambda_2 + \lambda_3)(\lambda_3 - \lambda_1)}}, \\ O_{12}^{(0)} &= -\sqrt{\frac{\lambda_1 \lambda_3 (\lambda_1 + \lambda_3)}{(\lambda_1 + \lambda_2)(\lambda_1 - \lambda_2 + \lambda_3)(\lambda_2 + \lambda_3)}}, \\ O_{13}^{(0)} &= \sqrt{\frac{\lambda_1 \lambda_2 (\lambda_2 - \lambda_1)}{(\lambda_3 - \lambda_1)(\lambda_1 - \lambda_2 + \lambda_3)(\lambda_2 + \lambda_3)}}, \\ O_{21}^{(0)} &= \sqrt{\frac{\lambda_1 (\lambda_3 - \lambda_2)}{(\lambda_1 + \lambda_2)(\lambda_3 - \lambda_1)}}, \\ O_{22}^{(0)} &= \sqrt{\frac{\lambda_2 (\lambda_1 + \lambda_3)}{(\lambda_1 + \lambda_2)(\lambda_2 + \lambda_3)}}, \\ O_{23}^{(0)} &= \sqrt{\frac{(\lambda_2 - \lambda_1) \lambda_3}{(\lambda_3 - \lambda_1)(\lambda_2 + \lambda_3)}}, \\ O_{31}^{(0)} &= -\sqrt{\frac{\lambda_1 (\lambda_2 - \lambda_1)(\lambda_1 + \lambda_3)}{(\lambda_1 + \lambda_2)(\lambda_3 - \lambda_1)(\lambda_1 - \lambda_2 + \lambda_3)}}, \\ O_{32}^{(0)} &= -\sqrt{\frac{\lambda_2 (\lambda_2 - \lambda_1)(\lambda_3 - \lambda_2)}{(\lambda_1 + \lambda_2)(\lambda_2 + \lambda_3)(\lambda_1 - \lambda_2 + \lambda_3)}}, \\ O_{33}^{(0)} &= \sqrt{\frac{\lambda_3 (\lambda_1 + \lambda_3)(\lambda_3 - \lambda_2)}{(\lambda_3 - \lambda_1)(\lambda_2 + \lambda_3)(\lambda_1 - \lambda_2 + \lambda_3)}},\end{aligned}\quad (7)$$

where the superscript “(0)” implies the Fritzsch (or $\epsilon_a = \epsilon_b = 0$) limit. Note that the above results hold for the normal mass hierarchy (i.e., $\lambda_1 < \lambda_2 < \lambda_3$)³.

Switching on the corrections of $\tilde{M}^{(\epsilon)}$ to $\tilde{M}^{(F)}$, one may calculate O and O' appearing in the bi-unitary transformation $O^\dagger \tilde{M}^{(NNI)} O' = \widehat{M}$ by following a perturbative way. We have done such a perturbative calculation both to the first order of ϵ_a and ϵ_b and to the second order of them, in order to examine whether the first-order analytical approximations are good enough. Of course, the fermion mass hierarchies should also be taken into account in our calculation. Given $m_e \ll m_\mu \ll m_\tau$, $m_u \ll m_c \ll m_t$ and $m_d \ll m_s \ll m_b$, it is easy to simplify Eq. (7) by making reliable analytical approximations. As only the normal hierarchy of three neutrino masses (i.e., $m_1 < m_2 < m_3$) is allowed in this scenario, it is also straightforward to simplify Eq. (7) in the neutrino sector. This treatment might not be excellent if three neutrinos have a relatively weak mass hierarchy, but it should be good enough for us to reveal the salient features of non-symmetric corrections to the Fritzsch textures. Our second-order analytical approximations in diagonalizing $\tilde{M}^{(NNI)} = \tilde{M}^{(F)} + \tilde{M}^{(\epsilon)}$, which include the $\mathcal{O}(\epsilon_a^2)$ and $\mathcal{O}(\epsilon_b^2)$ corrections, support the above arguments but they are too complicated to be presented here. To the first order of ϵ_a and ϵ_b , we simply take $O = O^{(0)}(\mathbf{1} + X)$ and $O' = O^{(0)}(\mathbf{1} - X)$ with X being anti-Hermitian (i.e., $X^\dagger = -X$) and proportional to the perturbation parameters ϵ_a and ϵ_b . In this case,

$$\begin{aligned}\tilde{M}^{(F)} &= O^{(0)} \widehat{M} O^{(0)\dagger}, \\ \tilde{M}^{(\epsilon)} &= O^{(0)} \left(X \widehat{M} + \widehat{M} X \right) O^{(0)\dagger}.\end{aligned}\tag{8}$$

Then we can determine the matrix elements of X in terms of those of $O^{(0)}$ and the perturbation parameters ϵ_a and ϵ_b . After an algebraic calculation, we obtain

$$\begin{aligned}O_{11} &= O_{11}^{(0)} \left[1 - \frac{\lambda_1 [(\lambda_1 - \lambda_2)^2 + (2\lambda_1 - \lambda_2)\lambda_3 + \lambda_3^2]}{(\lambda_1 - \lambda_2)(\lambda_1 + \lambda_3)(\lambda_1 - \lambda_2 + \lambda_3)} \epsilon_a + \frac{\lambda_1}{\lambda_1 - \lambda_2 + \lambda_3} \epsilon_b \right], \\ O_{12} &= O_{12}^{(0)} \left[1 - \frac{\lambda_2 [\lambda_1^2 + (\lambda_2 - \lambda_3)^2 - \lambda_1(2\lambda_2 - \lambda_3)]}{(\lambda_1 - \lambda_2)(\lambda_2 - \lambda_3)(\lambda_1 - \lambda_2 + \lambda_3)} \epsilon_a - \frac{\lambda_2}{\lambda_1 - \lambda_2 + \lambda_3} \epsilon_b \right], \\ O_{13} &= O_{13}^{(0)} \left[1 + \frac{[\lambda_1^2 - \lambda_1(\lambda_2 - 2\lambda_3) + (\lambda_2 - \lambda_3)^2] \lambda_3}{(\lambda_2 - \lambda_3)(\lambda_1 + \lambda_3)(\lambda_1 - \lambda_2 + \lambda_3)} \epsilon_a + \frac{\lambda_3}{\lambda_1 - \lambda_2 + \lambda_3} \epsilon_b \right], \\ O_{21} &= O_{21}^{(0)} \left[1 + \frac{\lambda_2 \lambda_3 (2\lambda_1 - \lambda_2 + \lambda_3)}{(\lambda_1 - \lambda_2)(\lambda_1 + \lambda_3)(\lambda_1 - \lambda_2 + \lambda_3)} \epsilon_a - \frac{\lambda_1}{\lambda_1 - \lambda_2 + \lambda_3} \epsilon_b \right], \\ O_{22} &= O_{22}^{(0)} \left[1 + \frac{\lambda_1 \lambda_3 (\lambda_1 - 2\lambda_2 + \lambda_3)}{(\lambda_1 - \lambda_2)(\lambda_2 - \lambda_3)(\lambda_1 - \lambda_2 + \lambda_3)} \epsilon_a + \frac{\lambda_2}{\lambda_1 - \lambda_2 + \lambda_3} \epsilon_b \right], \\ O_{23} &= O_{23}^{(0)} \left[1 - \frac{\lambda_1 \lambda_2 (\lambda_1 - \lambda_2 + 2\lambda_3)}{(\lambda_1 + \lambda_3)(\lambda_2 - \lambda_3)(\lambda_1 - \lambda_2 + \lambda_3)} \epsilon_a - \frac{\lambda_3}{\lambda_1 - \lambda_2 + \lambda_3} \epsilon_b \right], \\ O_{31} &= O_{31}^{(0)} \left[1 - \frac{\lambda_2 (\lambda_2 - \lambda_3) \lambda_3}{(\lambda_1 - \lambda_2)(\lambda_1 + \lambda_3)(\lambda_1 - \lambda_2 + \lambda_3)} \epsilon_a + \frac{\lambda_2 - \lambda_3}{\lambda_1 - \lambda_2 + \lambda_3} \epsilon_b \right], \\ O_{32} &= O_{32}^{(0)} \left[1 + \frac{\lambda_1 \lambda_3 (\lambda_1 + \lambda_3)}{(\lambda_1 - \lambda_2)(\lambda_2 - \lambda_3)(\lambda_1 - \lambda_2 + \lambda_3)} \epsilon_a - \frac{\lambda_1 + \lambda_3}{\lambda_1 - \lambda_2 + \lambda_3} \epsilon_b \right], \\ O_{33} &= O_{33}^{(0)} \left[1 - \frac{\lambda_1 (\lambda_1 - \lambda_2) \lambda_2}{(\lambda_2 - \lambda_3)(\lambda_1 + \lambda_3)(\lambda_1 - \lambda_2 + \lambda_3)} \epsilon_a - \frac{\lambda_1 - \lambda_2}{\lambda_1 - \lambda_2 + \lambda_3} \epsilon_b \right].\end{aligned}\tag{9}$$

³This mass hierarchy is consistent with both the observed mass spectra of charged fermions and the expected mass spectrum of neutrinos. Although an inverse mass hierarchy is also possible for three neutrinos, it cannot be consistent with the Fritzsch texture $M_\nu^{(F)}$ [10] or its non-Hermitian extension under discussion.

Given $\lambda_1 \ll \lambda_3$ and $\lambda_2 \ll \lambda_3$, the above expressions of O_{ij} (for $i, j = 1, 2, 3$) may approximate to

$$\begin{aligned}
O_{11} &\simeq \sqrt{\frac{\lambda_2}{\lambda_1 + \lambda_2}} \left(1 + \frac{\lambda_1}{\lambda_2 - \lambda_1} \epsilon_a + \frac{\lambda_1}{\lambda_3} \epsilon_b \right), \\
O_{12} &\simeq -\sqrt{\frac{\lambda_1}{\lambda_1 + \lambda_2}} \left(1 - \frac{\lambda_2}{\lambda_2 - \lambda_1} \epsilon_a - \frac{\lambda_2}{\lambda_3} \epsilon_b \right), \\
O_{13} &\simeq \sqrt{\frac{\lambda_1 \lambda_2 (\lambda_2 - \lambda_1)}{\lambda_3^3}} (1 - \epsilon_a + \epsilon_b), \\
O_{21} &\simeq \sqrt{\frac{\lambda_1 \lambda_3}{(\lambda_1 + \lambda_2)(\lambda_3 - \lambda_1 + \lambda_2)}} \left(1 - \frac{\lambda_2}{\lambda_2 - \lambda_1} \epsilon_a - \frac{\lambda_1}{\lambda_3} \epsilon_b \right), \\
O_{22} &\simeq \sqrt{\frac{\lambda_2 \lambda_3}{(\lambda_1 + \lambda_2)(\lambda_3 - \lambda_1 + \lambda_2)}} \left(1 + \frac{\lambda_1}{\lambda_2 - \lambda_1} \epsilon_a + \frac{\lambda_2}{\lambda_3} \epsilon_b \right), \\
O_{23} &\simeq \sqrt{\frac{\lambda_2 - \lambda_1}{\lambda_3 - \lambda_1 + \lambda_2}} (1 - \epsilon_b), \\
O_{31} &\simeq -\sqrt{\frac{\lambda_1 (\lambda_2 - \lambda_1)}{(\lambda_1 + \lambda_2)(\lambda_3 - \lambda_1 - \lambda_2)}} \left(1 - \frac{\lambda_2}{\lambda_2 - \lambda_1} \epsilon_a - \epsilon_b \right), \\
O_{32} &\simeq -\sqrt{\frac{\lambda_2 (\lambda_2 - \lambda_1)}{(\lambda_1 + \lambda_2)(\lambda_3 + \lambda_1 + \lambda_2)}} \left(1 + \frac{\lambda_1}{\lambda_2 - \lambda_1} \epsilon_a - \epsilon_b \right), \\
O_{33} &\simeq \sqrt{\frac{\lambda_3}{\lambda_3 - \lambda_1 + \lambda_2}} \left(1 + \frac{\lambda_2 - \lambda_1}{\lambda_3} \epsilon_b \right). \tag{10}
\end{aligned}$$

It is obvious that the off-diagonal matrix elements of O are more sensitive to the corrections induced by the perturbation parameters ϵ_a and ϵ_b .

3 A numerical illustration

Now let us take a look at how sensitive the flavor mixing parameters of leptons and quarks are to the perturbation parameters ϵ_a^α and ϵ_b^α (for $\alpha = u, d; l, \nu$). We first discuss the CKM matrix V and then analyze the MNSP matrix U in a numerical way.

(A) The CKM matrix V

Given six quark masses as the input parameters, the CKM matrix $V = O_u^\dagger P_V O_d$ still contains six free parameters: $\epsilon_a^u, \epsilon_b^u, \epsilon_a^d, \epsilon_b^d, \phi_1$ and ϕ_2 . Because the four perturbation parameters must be small, we require $|\epsilon_{a,b}^{u,d}| \lesssim 0.3$ as the reasonable bounds in our numerical calculation. Then the experimental data on four independent observable quantities of V , typically chosen as $|V_{us}|$, $|V_{cb}|$, $|V_{ub}|$ and $\sin 2\beta$ with $\beta \equiv \arg [-(V_{cd} V_{cb}^*) / (V_{td} V_{tb}^*)]$ being an inner angle of the CKM unitarity triangle [2], will allow us to constrain the parameter space of quark mass matrices $M_u^{(\text{NNI})}$ and $M_d^{(\text{NNI})}$. Such a constraint will be useful for model building.

To simplify the numerical calculation, we fix the values of quark masses at the electroweak scale $\mu = M_Z$ as follows: $m_u = 2.0$ MeV, $m_c = 0.557$ GeV, $m_t = 168.3$ GeV; $m_d = 2.7$ MeV, $m_s = 47$ MeV and $m_b = 2.92$ GeV [14, 12]. In addition, we adopt $|V_{us}| = 0.2255 \pm 0.0019$,

$|V_{cb}| = (41.2 \pm 1.1) \times 10^{-3}$, $|V_{ub}| = (3.93 \pm 0.36) \times 10^{-3}$ and $\sin 2\beta = 0.681 \pm 0.025$ [2]. By inputting the chosen values of six quark masses and allowing six free parameters of V to vary, one may then obtain the outputs of $|V_{us}|$, $|V_{cb}|$, $|V_{ub}|$ and $\sin 2\beta$ which are required to lie in their respective ranges given above. This treatment leads us to the parameter space of ϵ_a^u versus ϵ_b^u , ϵ_a^d versus ϵ_b^d and ϕ_1 versus ϕ_2 , as shown in Fig. 1. Some comments and discussions are in order ⁴.

(1) Although we have set the bounds $|\epsilon_{a,b}^{u,d}| \lesssim 0.3$, their allowed ranges are actually much smaller. In particular, $\epsilon_a^u \neq 0$ and $\epsilon_b^d \neq 0$ hold, but ϵ_b^u and ϵ_a^d are possible to vanish. This observation implies that both $M_u^{(\text{NNI})}$ and $M_d^{(\text{NNI})}$ must be non-Hermitian. On the other hand, one can see that $\epsilon_a^u < 0$ and $\epsilon_b^d > 0$ hold. In comparison, ϵ_b^u is negative in most cases and ϵ_a^d can be either positive or negative. To reduce the number of free parameters from four to two, one may either switch off ϵ_b^u and ϵ_a^d or set $\epsilon_a^u = \epsilon_b^u$ and $\epsilon_a^d = \epsilon_b^d$, or take $\epsilon_a^u = -\epsilon_b^d$ and $\epsilon_b^u = -\epsilon_a^d$, and so on. Such assumptions will strictly constrain the textures of quark mass matrices and might be suggestive for model building.

(2) It is impressive that two CP-violating phases ϕ_1 and ϕ_2 are restricted to a quite narrow parameter space. In particular, $|\phi_1| \sim 90^\circ$ and $|\phi_2| \sim 0^\circ$ imply that ϕ_1 dominates the strength of CP violation in the CKM matrix V . This feature is similar to the one showing up in some Hermitian modifications of the Fritzsch ansatz, such as the four-zero textures of quark mass matrices [15].

(3) In the quark sector we follow Ref. [12] to define the small parameter

$$\epsilon \equiv \frac{1}{2} \sqrt{(\epsilon_a^u)^2 + (\epsilon_b^u)^2 + (\epsilon_a^d)^2 + (\epsilon_b^d)^2} \quad (11)$$

to measure the overall non-Hermitian departure of $M_u^{(\text{NNI})}$ and $M_d^{(\text{NNI})}$ from the Fritzsch texture. The Jarlskog invariant of CP violation [16], defined as \mathcal{J} for the CKM matrix V , can be calculated via $\mathcal{J} = \text{Im}(V_{us}V_{cb}V_{ub}^*V_{cs}^*)$. We illustrate the numerical dependence of \mathcal{J} on ϵ in Fig. 2, where $\mathcal{J} \sim 3.7 \times 10^{-5}$ for $\epsilon \sim 0.2$. The sign of \mathcal{J} is fixed by that of $\sin 2\beta$.

(B) The MNSP matrix U

Given three charged-lepton masses and two neutrino mass-squared differences $\Delta m_{21}^2 \equiv m_2^2 - m_1^2$ and $\Delta m_{32}^2 \equiv m_3^2 - m_2^2$, the MNSP matrix $U = O_l^\dagger P_U O_\nu$ depends on seven free parameters: ϵ_a^l , ϵ_b^l , ϵ_a^ν , ϵ_b^ν , m_1 , φ_1 and φ_2 . Again we require $|\epsilon_{a,b}^{l,\nu}| \lesssim 0.3$ as the reasonable bounds. The present neutrino oscillation data on three flavor mixing angles, denoted as θ_{12} , θ_{13} and θ_{23} in the standard parametrization of U (i.e., $\tan \theta_{12} = |U_{e2}/U_{e1}|$, $\sin \theta_{13} = |U_{e3}|$ and $\tan \theta_{23} = |U_{\mu 3}/U_{\tau 3}|$) [2], will allow us to constrain the parameter space of lepton mass matrices $M_l^{(\text{NNI})}$ and $M_\nu^{(\text{NNI})}$. For simplicity, we fix the values of three charged-lepton masses at the electroweak scale as follows: $m_e = 0.48657$ MeV, $m_\mu = 102.718$ MeV and $m_\tau = 1746.24$ MeV [14]. Moreover, we assume $m_1 = 0.0025$ eV and take $\Delta m_{21}^2 = 8.0 \times 10^{-5}$ eV² and $\Delta m_{32}^2 = 2.5 \times 10^{-3}$ eV² together with $30^\circ < \theta_{12} < 38^\circ$, $36^\circ < \theta_{23} < 54^\circ$ and $\theta_{13} < 10^\circ$ in our numerical calculation. Then the normal but weak neutrino mass hierarchy is measured by two mass ratios $m_1/m_2 \simeq 0.27$ and $m_2/m_3 \simeq 0.18$. By inputting the chosen values of charged-lepton and neutrinos masses and allowing the unknown parameters of U to vary, one may obtain the outputs of θ_{12} , θ_{13} and θ_{23} which are required to lie in their respective ranges given above. This treatment leads us to the parameter space of ϵ_a^l versus ϵ_b^l , ϵ_a^ν versus ϵ_b^ν and φ_1 versus φ_2 , as shown in Fig. 3. Some comments and discussions are in order.

⁴Note that Branco *et al* have recently analyzed the CKM matrix V in such a way [12]. Our more comprehensive analysis not only confirms their results but also provides ourselves with a meaningful calibration as we extend the same analysis to the lepton sector. Our results for the MNSP matrix U in section 3 (B) are completely new.

(1) Because of $m_e/m_\mu \ll m_1/m_2$ and $m_\mu/m_\tau \ll m_2/m_3$, the MNSP matrix U is expected to receive more contributions from the neutrino sector rather than the charged-lepton sector. That is why the bounds on $|\epsilon_{a,b}^l|$ are much looser than those on $|\epsilon_{a,b}^{\nu}|$, as one can see from Fig. 3. We find that ϵ_a^ν and ϵ_b^ν are negative in most cases. To reduce the number of free parameters from four to two, one may simply switch off ϵ_a^l and ϵ_b^l . Although it is also possible to set $\epsilon_a^\nu = \epsilon_b^\nu = 0$, it will be impossible to get $\theta_{23} \simeq 45^\circ$ for the atmospheric neutrino mixing angle [10]. More precise data to be extracted from the upcoming neutrino oscillation experiments may help us constrain the ranges of $\epsilon_{a,b}^l$ and $\epsilon_{a,b}^\nu$ to a better degree of accuracy.

(2) Current neutrino oscillation experiments set no constraint on the CP-violating phase φ_1 . But the other CP-violating phase φ_2 is well restricted to be around 180° , as shown in Fig. 3. The reason is simply that a sufficiently large value of θ_{23} requires $\varphi_2 \sim 180^\circ$. To see this point more clearly, we write out

$$\tan \theta_{23} = \left| \frac{U_{\mu 3}}{U_{\tau 3}} \right| \simeq \left| \frac{h_l (1 - \epsilon_b^l) - h_\nu (1 - \epsilon_b^\nu) e^{i\varphi_2}}{(1 + h_l^2 \epsilon_b^l + h_\nu^2 \epsilon_b^\nu) + h_l h_\nu (1 - \epsilon_b^l) (1 - \epsilon_b^\nu) e^{i\varphi_2}} \right| \quad (12)$$

with the help of Eq. (10), where $h_l \equiv \sqrt{(m_\mu - m_e)/m_\tau} \simeq \sqrt{m_\mu/m_\tau}$ and $h_\nu \equiv \sqrt{(m_2 - m_1)/m_3}$. It becomes transparent that $\varphi_2 \sim 180^\circ$, together with $\epsilon_b^l < 0$ and $\epsilon_b^\nu < 0$, may enhance the magnitude of $\tan \theta_{23}$ and make θ_{23} closer to its best-fit value (i.e., $\theta_{23} \simeq 45^\circ$).

(3) Similar to the definition of ϵ in the quark sector, a small parameter

$$\epsilon' \equiv \frac{1}{2} \sqrt{(\epsilon_a^l)^2 + (\epsilon_b^l)^2 + (\epsilon_a^\nu)^2 + (\epsilon_b^\nu)^2} \quad (13)$$

can also be defined to measure the overall non-Hermitian departure of $M_l^{(\text{NNI})}$ and $M_\nu^{(\text{NNI})}$ from the Fritzsch texture. We illustrate the dependence of three flavor mixing angles on ϵ' in Fig. 4. The Jarlskog invariant of leptonic CP violation, which can be calculated via $\mathcal{J}' = \text{Im}(U_{e2}U_{\mu 3}U_{e3}^*U_{\mu 2}^*)$, is also shown in Fig. 4. We see that it is possible to reach $|\mathcal{J}'| \sim 1.5 \times 10^{-2}$. The CP-violating effects at this level should be observable in the future long-baseline neutrino oscillation experiments.

Finally, it makes sense to compare between the MNSP and CKM matrices derived from the same NNI textures of lepton and quark mass matrices. Given $|\epsilon_{a,b}^{u,d}| \lesssim 0.3$ and $|\epsilon_{a,b}^{l,\nu}| \lesssim 0.3$, it can be concluded that the smallness of three quark mixing angles is primarily attributed to the strong mass hierarchies of up- and down-type quarks, while the largeness of solar and atmospheric neutrino mixing angles is mainly ascribed to the relatively weak hierarchy of three neutrino masses. Of course, the CP-violating phases play an important role in either the lepton sector or the quark sector. Note that V_{ub} is smaller in magnitude than all the other elements of the CKM matrix V , and U_{e3} is also the smallest element of the MNSP matrix U . In other words, θ_{13} is the smallest mixing angle in both lepton and quark sectors. This interesting feature is a natural consequence of the flavor textures of leptons and quarks together with their corresponding mass hierarchies. In addition, the fact that $|\epsilon_{a,b}^{u,d}| \sim |\epsilon_{a,b}^{l,\nu}| \sim 0.2$ is favored by current experimental data should be quite suggestive of a unified flavor model of leptons and quarks.

4 Summary

We have introduced non-Hermitian and nearest-neighbor-interacting perturbations to the Fritzsch textures of lepton and quark mass matrices such that both of them can fit current experimental

data very well. In particular, we find that it is possible to obtain $\theta_{23} \simeq 45^\circ$ for the atmospheric neutrino mixing angle and predict $\theta_{13} \simeq 3^\circ$ to 6° for the smallest neutrino mixing angle when the dimensionless perturbation parameters in the lepton sector are at the 20% level. We have shown that the same level of perturbations is required in the quark sector, where the Jarlskog invariant of CP violation is about 3.7×10^{-5} . In comparison, the strength of leptonic CP violation is likely to reach about 1.5×10^{-2} in neutrino oscillations.

As shown in Ref. [12], the NNI texture of quark mass matrices can be derived from the introduction of an Abelian flavor symmetry (e.g., the minimal realization of this idea requires a Z_4 flavor symmetry in the context of a two-Higgs doublet model). We can follow the same procedure to obtain the NNI texture of lepton mass matrices if massive neutrinos are the Dirac particles. In the presence of a few heavy Majorana neutrinos, one may first impose the aforementioned flavor symmetry on the Yukawa interaction of neutrinos to get the NNI texture for the Dirac neutrino mass matrix and then achieve the Majorana mass matrix for three light neutrinos via the seesaw mechanism. There are therefore a number of possibilities of model building, but the numerical results must be very different from what we have presented in this work. One may explore such possibilities once more accurate experimental data on neutrino masses and lepton flavor mixing angles are available in the (near) future, and in particular when the simple scenario discussed in this paper is phenomenologically discarded or becomes less favored.

Let us reiterate that a parallel study of lepton and quark mass matrices, such as the approximate Fritzsch textures under discussion, is useful to reveal the similarities and differences between the lepton and quark sectors. It should also be helpful for building a unified flavor model of leptons and quarks with the help of proper flavor symmetries.

This work was supported in part by the National Natural Science Foundation of China under grant No. 10875131 and in part by the Ministry of Science and Technology of China under grant No. 2009CB825207.

References

- [1] N. Cabibbo, Phys. Rev. Lett. **10**, 531 (1963); M. Kobayashi and T. Maskawa, Prog. Theor. Phys. **49**, 652 (1973).
- [2] Particle Data Group, K. Nakamura *et al.*, J. Phys. G **37**, 075021 (2010).
- [3] Z. Maki, M. Nakagawa, and S. Sakata, Prog. Theor. Phys. **28**, 870 (1962); B. Pontecorvo, Sov. Phys. JETP **26**, 984 (1968).
- [4] For recent reviews with extensive references, see: H. Fritzsch and Z.Z. Xing, Prog. Part. Nucl. Phys. **45**, 1 (2000); A. Strumia and F. Vissani, hep-ph/0606054; K.S. Babu, arXiv:0910.2948.
- [5] S. Weinberg, Trans. New York Acad. Sci. **38**, 185 (1977); F. Wilczek and A. Zee, Phys. Lett. B **70**, 418 (1977); H. Fritzsch, Phys. Lett. B **70**, 436 (1977).
- [6] H. Fritzsch, Phys. Lett. B **73**, 317 (1978); Nucl. Phys. B **155**, 189 (1979).
- [7] G.C. Branco, L. Lavoura, and F. Mota, Phys. Rev. D **39**, 3443 (1989).

- [8] This approach has been extensively studied in the past two decades. For a recent comprehensive work with many references, see: G. Couture, C. Hamzaoui, S.S.Y. Lu, and M. Toharia, *Phys. Rev. D* **81**, 033010 (2010).
- [9] G.C. Branco and F. Mota, *Phys. Lett. B* **280**, 109 (1992); K. Harayama and N. Okamura, *Phys. Lett. B* **387**, 614 (1996); T. Ito and M. Tanimoto, *Phys. Rev. D* **55**, 1509 (1997); Y. Koide, *Mod. Phys. Lett. A* **12**, 2655 (1997); K. Harayama, N. Okamura, A.I. Sanda, and Z.Z. Xing, *Prog. Theor. Phys.* **97**, 781 (1997); E. Takasugi and M. Yoshimura, *Prog. Theor. Phys.* **98**, 1313 (1997); T. Ito, N. Okamura, and M. Tanimoto, *Phys. Rev. D* **58**, 077301 (1998); Z. Berezhiani and A. Rossi, *JHEP* **9903**, 002 (1999); K. Hagiwara and N. Okamura, *Nucl. Phys. B* **548**, 60 (1999); G. Altarelli and F. Feruglio, *Phys. Lett. B* **451**, 388 (1999); D. Dooling and K. Kang, *Phys. Lett. B* **455**, 264 (1999); S. Falk, R. Haussling, and F. Scheck, *Phys. Rev. D* **65**, 093011 (2002); G.C. Branco, M.N. Rebelo, and J.I. Silva-Marcos, *Phys. Lett. B* **597**, 155 (2004); *Phys. Rev. D* **76**, 033008 (2007); T. Fukuyama, K. Matsuda, and H. Nishiura, *Int. J. Mod. Phys. A* **22**, 5325 (2007); K.S. Babu and Y. Meng, *Phys. Rev. D* **80**, 075003 (2009); G.C. Branco, D. Emmanuel-Costa, and C. Simões, *Phys. Lett. B* **690**, 62 (2010).
- [10] Z.Z. Xing, *Phys. Lett. B* **550**, 178 (2002); Z.Z. Xing and S. Zhou, *Phys. Lett. B* **593**, 156 (2004); M. Randhawa, G. Ahuja, and M. Gupta, *Phys. Lett. B* **643**, 175 (2006).
- [11] M. Fukugita, M. Tanimoto, and T. Yanagida, *Phys. Lett. B* **562**, 273 (2003); S. Zhou and Z.Z. Xing, *Eur. Phys. J. C* **38**, 495 (2005); M. Obara and Z.Z. Xing, *Phys. Lett. B* **644**, 136 (2007).
- [12] G.C. Branco, D. Emmanuel-Costa, and C. Simões, in Ref. [9].
- [13] H. Georgi and S.L. Nanopoulos, *Nucl. Phys. B* **155**, 52 (1979).
- [14] Z.Z. Xing, H. Zhang, and S. Zhou, *Phys. Rev. D* **77**, 113016 (2008).
- [15] See, e.g., H. Fritzsch and Z.Z. Xing, *Phys. Lett. B* **353**, 114 (1995); *Nucl. Phys. B* **556**, 49 (1999); *Phys. Lett. B* **555**, 63 (2003).
- [16] C. Jarlskog, *Phys. Rev. Lett.* **55**, 1039 (1985).

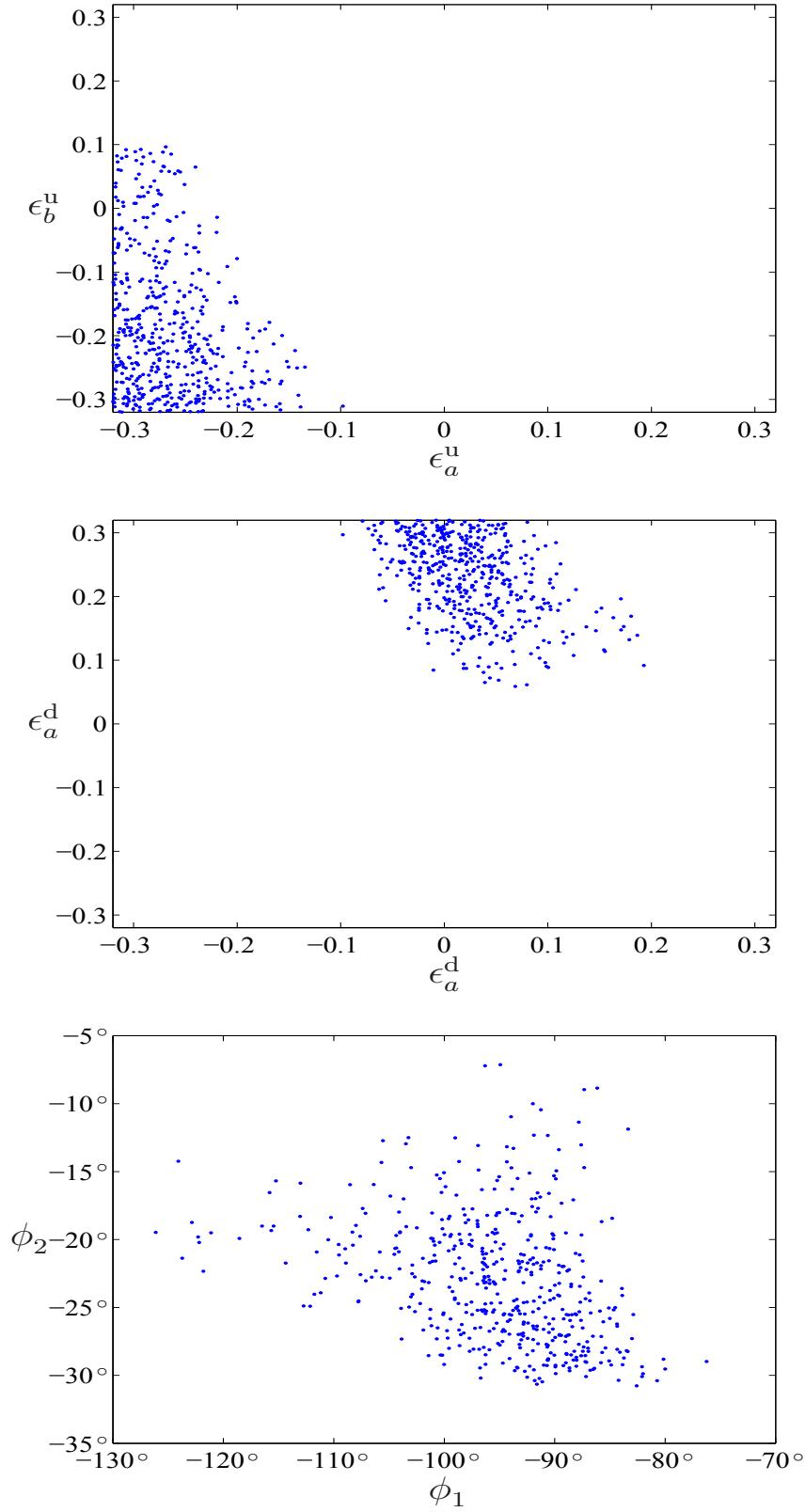


Figure 1: An illustration of the parameter space of ϵ_a^u versus ϵ_b^u , ϵ_a^d versus ϵ_b^d and ϕ_1 versus ϕ_2 constrained by current data in the quark sector.

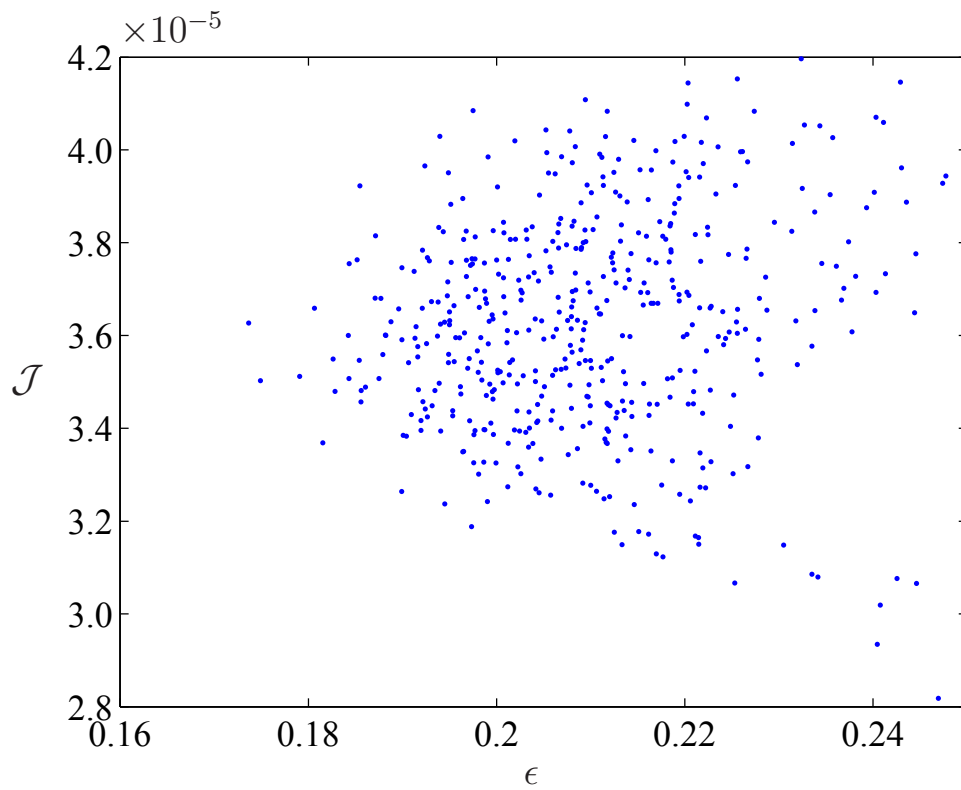


Figure 2: An illustration of the dependence of the Jarlskog invariant of CP violation \mathcal{J} on the overall perturbation parameter ϵ in the quark sector.

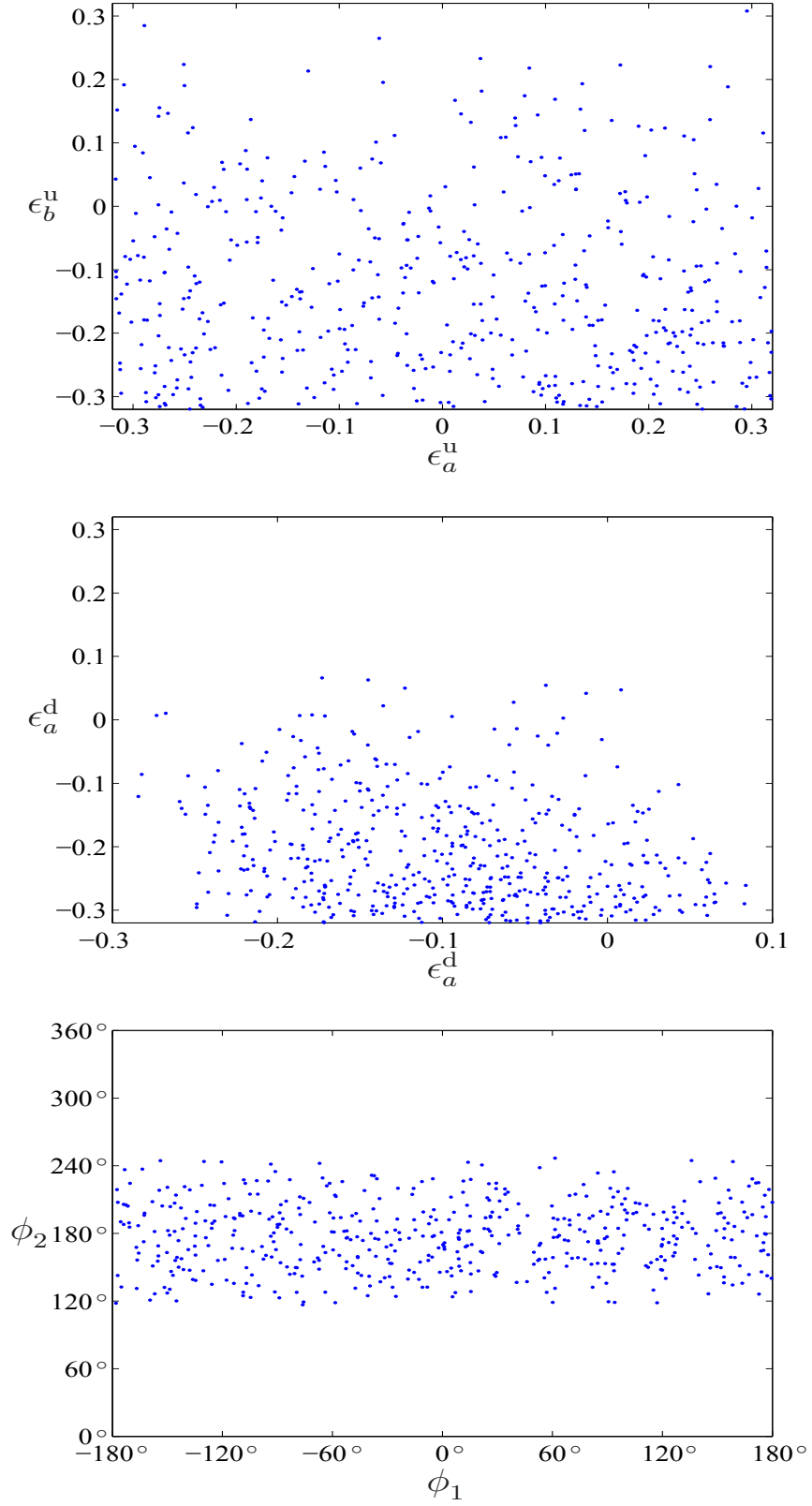


Figure 3: An illustration of the parameter space of ϵ_a^l versus ϵ_b^l , ϵ_a^ν versus ϵ_b^ν and φ_1 versus φ_2 in the lepton sector with the input $m_1 = 0.0025$ eV.

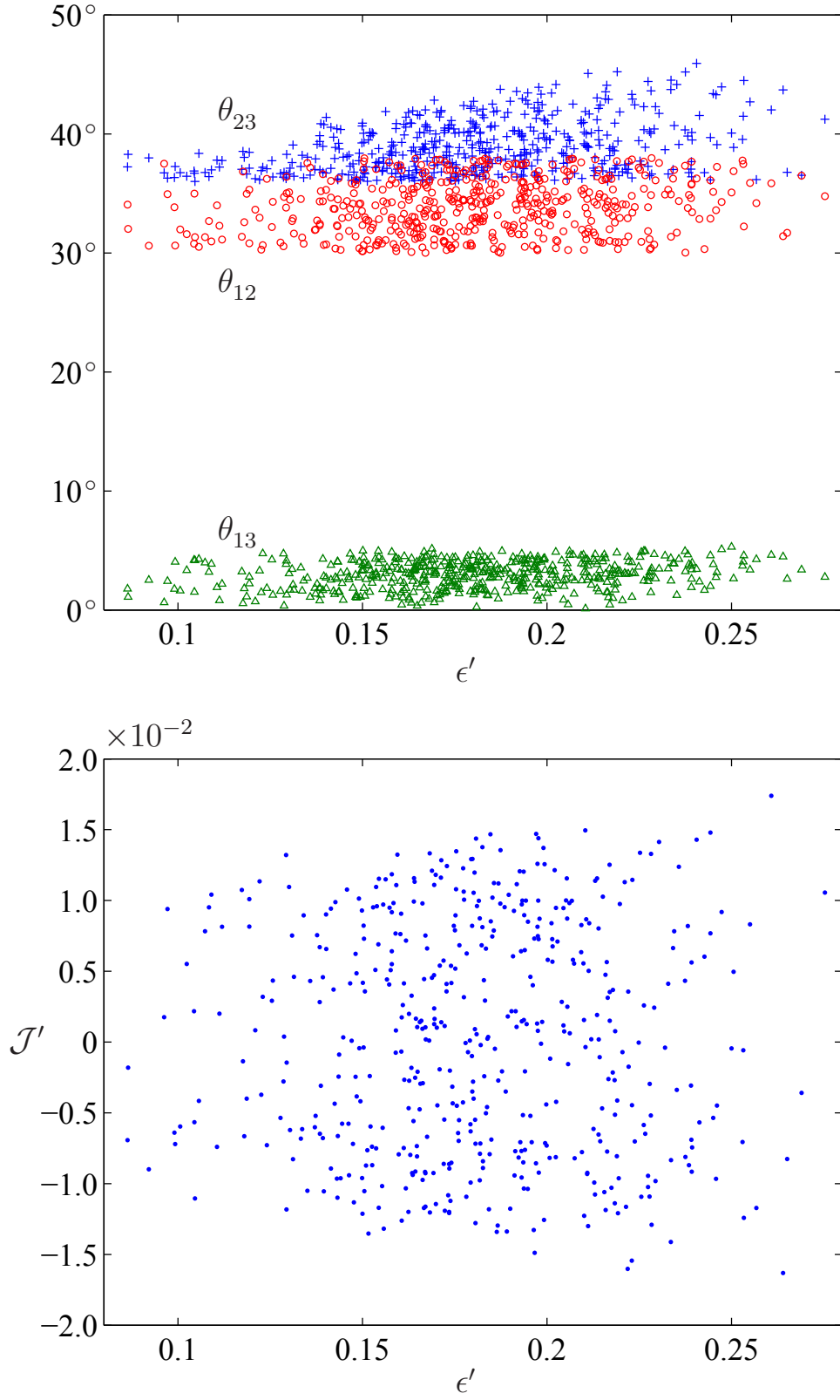


Figure 4: An illustration of the dependence of three flavor mixing angles and the Jarlskog invariant of CP violation \mathcal{J}' on the overall perturbation parameter ϵ' in the lepton sector.